Mechanism of the Reaction Catalyzed by Mandelate Racemase: Structure and Mechanistic Properties of the D270N Mutant[†,‡]

Susan L. Schafer, William C. Barrett,[§] Abraham T. Kallarakal, Bharati Mitra, John W. Kozarich,[||] and John A. Gerlt*,[§]

Department of Chemistry and Biochemistry, University of Maryland, College Park, Maryland 20742, and Department of Biochemistry, University of Illinois, Urbana, Illinois 61801

James G. Clifton and Gregory A. Petsko*

Rosensteil Center for Biomedical Sciences, Brandeis University, Waltham, Massachusetts 02254

George L. Kenyon

Department of Pharmaceutical Chemistry, School of Pharmacy, University of California, San Francisco, California 94143

Received January 24, 1996[⊗]

ABSTRACT: On the basis of the available high-resolution structures of mandelate racemase (MR) from *Pseudomonas putida* [Landro, J. A., Gerlt, J. A., Kozarich, J. W., Koo, C. W., Shah, V. J., Kenyon, G. L., Neidhart, D. J., Fujita, J., & Petsko, G. A. (1994) *Biochemistry 33*, 635−643], Lys 166 and His 297 are positioned appropriately to participate in catalysis as acid/base catalysts, with Lys 166 participating as the (*S*)-specific acid/base catalyst and His 297 participating as the (*R*)-specific acid/base catalyst. The dependence of k_{cat} on pH for the racemization of both (*R*)- and (*S*)-mandelates suggests that the pK_as of the conjugate acids of Lys 166 and His 297 are both ∼6.4 [Landro, J. A., Kallarakal, A. T., Ransom, S. C., Gerlt, J. A., Kozarich, J. W., Neidhart, D. J., & Kenyon, G. L. (1991) *Biochemistry 30*, 9274−9281; Kallarakal, A. T., Mitra, B., Kozarich, J. W., Gerlt, J. A., Clifton, J. R., Petsko, G. A., & Kenyon, G. L. (1995) *Biochemistry 34*, 2788−2797]. Both acid/base catalysts are in close proximity to and approximately equidistant to the ϵ-ammonium group of Lys 164 and the essential Mg^{2+}. The positive electrostatic potential provided by these cationic groups might be expected to increase the acidities of the cationic conjugate acids of the acid/base catalysts, thereby explaining the depressed pK_a of Lys 166 but not the "normal" pK_a of His 297. Asp 270 is hydrogen bonded to N^{δ} of His 297 and, therefore, may allow the pK_a of His 297 to be normal. In this paper we report the structural and mechanistic properties of the mutant in which Asp 270 is replaced with asparagine (D270N). The structure of D270N with (*S*)-atrolactate bound in the active site reveals no geometric alterations in the active site when compared to the structure of wild-type MR complexed with (*S*)-atrolactate, with the exception that the side chain of His 297 is tilted and displaced ∼0.5 Å away from Asn 270 and toward the (*S*)-atrolactate. The k_{cat}s for both (*R*)- and (*S*)-mandelates are reduced ∼10^4-fold. In accord with the proposal that Asp 270 influences the pK_a of His 297, in the (*R*)- to (*S*)-direction no ascending limb is detected in the dependence of k_{cat} on pH; instead, k_{cat} decreases from a low pH plateau as described by a pK_a of 10. In the (*S*)- to (*R*)-direction the dependence of k_{cat} on pH is a bell-shaped curve that is described by pK_as of 6.4 and 10. In analogy to the previously reported properties of the H297N mutant [Landro, J. A., Kallarakal, A. T., Ransom, S. C., Gerlt, J. A., Kozarich, J. W., Neidhart, D. J., & Kenyon, G. L. (1991) *Biochemistry 30*, 9274−9281], D270N catalyzes both the facile exchange of the α-proton of (*S*)- but not (*R*)-mandelate with solvent and the stereospecific elimination of bromide ion from (*S*)-*p*-(bromomethyl)mandelate. These observations suggest that His 297 and Asp 270 function as a catalytic dyad, with Asp 270 being at least partially responsible for the normal pK_a of His 297 in wild-type MR.

Mandelate racemase (MR;[1] EC 5.1.2.2) from *Pseudomonas putida* ATCC 12633 catalyzes the interconversion of the (*R*)- and (*S*)-enantiomers of mandelate (Kenyon & Hegeman, 1979; Gerlt et al., 1992). On the basis of the high-resolution X-ray structure of wild-type MR (Neidhart et al., 1991), Lys 166 and His 297 were proposed to be the general acid/general base catalysts that transfer protons to and from the α-carbons of the substrate and product enantiomers. Lys 166 is appropriately positioned in the active site to act as the (*S*)-specific acid/base catalyst while His 297 is appropriately

[†] This is paper 20 in a series on mandelate racemase; paper 19 is Kallarakal et al. (1995). This research was supported by Grant GM-40570 (J.A.G., G.L.K., J.W.K., and G.A.P.) from the National Institutes of Health.

[‡] X-ray coordinates for the D270N mutant of mandelate racemase have been deposited in the Brookhaven Protein Data Bank with the File Name 1MRA.

[§] Present address: Department of Biochemistry, University of Illinois, 419 Roger Adams Laboratory, 600 South Mathews Ave., Urbana, IL 61801.

[||] Present address: Department of Biochemistry, Merck Research Laboratories, P.O. Box 2000, Rahway, NJ 07065-0900.

[⊗] Abstract published in *Advance ACS Abstracts,* April 15, 1996.

[1] Abbreviations: CAPS, 3-(cyclohexylamino)-1-propanesulfonic acid; CHES, 2-(cyclohexylamino)-1-ethanesulfonic acid; HEPES, 4-(2-hydroxyethyl)piperazine-1-ethanesulfonic acid; LB, Luria broth; MES, 2-(*N*-morpholino)ethanesulfonic acid; MR, mandelate racemase; PIPES, piperazine-1,4-bis(2-ethanesulfonic acid); TAPS, *N*-[tris(hydroxymethyl)methyl]-3-aminopropanesulfonic acid.

S0006-2960(96)00174-2 CCC: $12.00

positioned to act as the (*R*)-specific acid/base catalyst.

The role of Lys 166 in catalysis has been investigated by both chemical modification studies (Landro et al., 1994) and structural and mechanistic examination of the K166R mutant of MR (Kallarakal et al., 1995). The results of both of these studies support the proposal that Lys 166 is the (*S*)-specific acid/base catalyst. This assignment is in accord with the observed incorporation of solvent deuterium into the (*S*)-enantiomer of mandelate during the course of the racemization reaction (Powers et al., 1991).

In contrast, no incorporation of solvent deuterium into the (*R*)-enantiomer of mandelate was observed during the course of racemization. Such behavior would be expected if His 297 were the (*R*)-specific base as suggested by the crystallographic analysis. The role of His 297 in catalysis has been investigated by structural and mechanistic examination of the H297N mutant of MR. This mutant is unable to racemize either enantiomer of mandelate. However, the H297N mutant is able to catalyze both the stereospecific elimination of bromide ion from the (*S*)-enantiomer of (*R*,*S*)-*p*-(bromomethyl)mandelate and the exchange of the α-proton of (*S*)- but not (*R*)-mandelate with solvent hydrogen (Landro et al., 1991). These experiments support the proposal that His 297 is the (*R*)-specific acid/base catalyst.

The dependence of k_{cat} on pH for the racemization of both (*R*)- and (*S*)-mandelates was also reported by Landro et al. (1991). For each enantiomer, the pH dependence of k_{cat} is described by a bell-shaped curve, thereby suggesting the participation of two ionizable groups: a basic catalyst with a pK_a of ∼6.4 and an acidic catalyst with a pK_a of ∼10.0. The pK_a values for the catalysts are identical, within experimental error, using either (*R*)- or (*S*)-mandelate as substrate. When (*R*)-mandelate is substrate, the pK_a of 6.4 tentatively was assigned to the imidazolium group of His 297 (the conjugate acid of the general base catalyst) and the pK_a of 10.0 tentatively was assigned to ϵ-ammonium group of Lys 166 (the general acid catalyst). Analogously, when (*S*)-mandelate is substrate, the pK_a of 6.4 tentatively was assigned to the ϵ-ammonium group of Lys 166 (the conjugate acid of the general base catalyst) and the pK_a of 10.0 tentatively was assigned to the imidazolium group of His 297 (the general acid catalyst). However, the dependence of k_{cat} on pH observed for the K166R mutant of MR (Kallarakal et al., 1995) leads to the conclusion that while the pK_a of the ascending limb of the dependence of k_{cat} on pH may be associated with the conjugate acid of the general base catalyst, the pK_a of the descending limb is not likely associated with the general acid catalyst. The evidence for this suggestion was that the K166R mutant was observed to increase only the pK_a of the ascending limb (by ≥1.6 pK_a units) when (*S*)-mandelate was used as substrate.[2]

The observed pK_a of ∼6.4 for the conjugate acid of the general base catalyst when (*R*)-mandelate is substrate (His 297) is characteristic of the imidazolium group of histidine in solution (Creighton, 1993). However, this pK_a value for the conjugate acid of the general base catalyst when (*S*)-mandelate is substrate (Lys 166) is not characteristic of the ϵ-ammonium group of lysine in solution.

[2] These tentative assignments were made with the knowledge that the dependence of kinetic parameters on pH do not necessarily reflect the microscopic pK_as of functional groups in enzyme active sites (Bruice & Schmir, 1959; Schmidt & Westheimer, 1971; Knowles, 1976).

The X-ray structures of (1) wild-type MR complexed with the competitive inhibitor (*S*)-atrolactate (Landro et al., 1994), (2) wild-type MR inactivated by alkylation of the ϵ-amino group of Lys 166 with (*R*)-α-phenylglycidate (Landro et al., 1994), (3) the E317Q mutant complexed with (*S*)-atrolactate (Mitra et al., 1995), and (4) the K166R mutant complexed with the substrate (*S*)-mandelate (Kallarakal et al., 1995) all reveal that both the ϵ-ammonium group of Lys 166 and the imidazolium group of His 297 are in close proximity to and approximately equidistant from the ϵ-ammonium group of Lys 164 and the essential Mg^{2+}. The proximity of these charged groups to both the ϵ-ammonium group of Lys 166 and the imidazolium group of His 297 might be expected to enhance the acidities of these cationic acids. For example, in the active site of acetoacetate decarboxylase, the presumed close proximity of the ϵ-ammonium groups of two adjacent lysine residues (Lys 115 and 116; Laursen & Westheimer, 1966; Petersen & Bennett, 1990) has been proposed to provide electrostatic destabilization which decreases the pK_a of the ϵ-ammonium group of Lys 115 to 5.9 (Kokesh & Westheimer, 1971); support for this proposal has recently been obtained by studies of various site-directed mutants for Lys 115 and Lys 116 (Highbarger et al., 1996). The ϵ-amino group of Lys 115 forms a Schiff base with the substrate, so this increase in acidity enhances its nucleophilicity at pH 6, the pH optimum of the decarboxylase.

While the pK_a of the ϵ-ammonium group of Lys 166 is apparently decreased by the positive electrostatic environment of the active site of MR, the pK_a of the imidazolium group of His 297 is unperturbed. The "normal" pK_a of His 297 suggests that an anionic group may be spatially proximal, thereby negating the positive electrostatic potential provided by the ϵ-ammonium group of Lys 164 and the essential Mg^{2+}. The four available X-ray structures of MR and its mutants all reveal that the carboxylate group of Asp 270 is hydrogen bonded to N^{δ} of His 297.

In this article we describe the structural and mechanistic characterization of the D270N mutant of MR. A high-resolution structure of D270N has been obtained with (*S*)-atrolactate bound in the active site. Although the position of the C^{α} of Asn 270 is unchanged from that of Asp 270 in the active site of wild-type MR, the side chain of His 297 is rotated and displaced toward the binding site for the (*S*)-atrolactate. The k_{cat}s for the racemization of both enantiomers of mandelate are decreased ∼10^4-fold by the Asp to Asn substitution, and the dependencies of the k_{cat}s on pH are those expected if Asp 270 influences the pK_a of His 297. The significant decrease in k_{cat} suggests that His 297 and Asp 270 function together as a catalytic dyad.

MATERIALS AND METHODS

Materials. Restriction endonucleases, bacteriophage T4 DNA ligase, and bacteriophage T4 polynucleotide kinase were purchased from Boehringer Mannheim. Calf intestine alkaline phosphatase was from Pharmacia LKB. Site-directed mutagenesis was performed by the phosphorothioate method using a kit obtained from Amersham. DNA sequence analysis was performed with the Sequenase kit from U.S. Biochemicals. Synthetic oligonucleotides used for the mutagenesis and DNA sequencing were purchased from the Protein Nucleic Acid Laboratory, University of Maryland, College Park, and from Oligo's Etc., Wilsonville, OR.

Plasmid DNA was isolated and purified from bacterial cultures using the reagents and instructions from the Promega Magic Miniprep kit. The Bio101 GeneClean kit was used for all other DNA isolation and purification steps. The techniques described by Sambrook et al. (1989) were used for cloning and for both DNA and protein gel electrophoresis.

(*R*,*S*)-*p*-(Bromomethyl)mandelate was synthesized following the procedure of Lin et al. (1988).

[α-^{2}H]-(*R*)-Mandelate was prepared by fractional recrystallization of diastereomeric salts of racemic [α-^{2}H]mandelic acid that was synthesized using wild-type MR to catalyze the exchange of substrate protium with solvent deuterium (Mitra et al., 1995).

[α-^{2}H]-(*S*)-Mandelate was synthesized from [α-^{1}H]-(*S*)-mandelate using H297N to catalyze the exchange of substrate protium with solvent deuterium (Landro et al., 1991).

Site-Directed Mutagenesis. The template for mutagenesis was M13mp18 into which the 1.9 kb *Eco*RV-*Sst*I fragment of pMRαpg (Tsou et al., 1989) containing the entire gene for MR had been cloned (Landro et al., 1991). The synthetic 33-mer d(GCTATGCCAAACGCAATGAAGATCGGTGGCGTG) was used to construct the D270N mutant, where the positions of the mismatches are indicated by the underlined bases. The entire mutant gene was sequenced by using a series of synthetic primers to verify that no other alterations in nucleotide sequence had occurred.

Purification of the D270N Mutant. The gene for D270N along with the *trc* promoter was cloned into the broad-host range vector pKT230 as previously described (Landro et al., 1991). The plasmid containing the gene for D270N was designated pKTtrc/D270N. *Pseudomonas aeruginosa* (ATCC 15692) was transformed with pKTtrc/D270N and grown in LB media containing 1 mg/mL streptomycin. The mutant protein was purified according to the procedure described by Tsou et al. (1989). Since D270N had very low racemase activity, SDS−PAGE was used to monitor column fractions for the D270N protein.

Crystallization of D270N. D270N was cocrystallized with the inhibitor (S)-atrolactate using the procedures described previously (Mitra et al., 1995). Crystals appeared after 2 days and were fully grown within 1 week. Suitable single crystals were mounted directly from the hanging drop shortly before data collection.

Data Collection. All data were collected from a single crystal using a Siemens multiwire detector mounted on an Elliot GX-6 rotating anode generator, operated with a fine-focus cup at approximately 30 kV and 25 mA. To minimize radiation-induced damage, a cold air stream maintained the crystal temperature at approximately 4 °C. Data frames were processed using the XDS program (Kabsch, 1988a,b). Two different orientations were collected and merged using the program XSCALE (Kabsch, 1988b). The space group and unit cell parameters were isomorphous to those of wild-type MR (I422; 125.0 × 125.0 × 107.1 Å). The merged 2.0 Å data set had an overall merging *R* factor of 17% on intensity. On the basis of both the statistics of the merging *R* factor *vs* resolution and the completeness of the data *vs* signal-to-noise (σ) ratio, the data set used for refinement contained 19 219 reflections from 20.0 to 2.1 Å resolution that have intensities greater than 1σ (Table 1).

Structure Refinement. The initial difference electron density maps calculated using these data and the phases from the refined structure of wild-type MR indicated that there were no gross rearrangements: all of the active site residues (Lys 166, Asp 195, Glu 221, Glu 247, His 297, and Glu 317), Asn 270, the magnesium ion, and the inhibitor fit clearly into the electron density map. However, the density for amino acids 18 through 32 (the "flap" that closes over the active site to exclude solvent) was poor. Therefore, the initial model for refinement was the wild-type structure lacking these residues. Additionally, Asn 270 and the remaining active site residues listed previously were represented as alanines (to debias the phases) and without water molecules, the inhibitor, or the magnesium ion present.

Table 1: Data Collection Statistics from XSCALE

high-resolution limit (Å)	*R* factor (%) orientation 1	*R* factor (%) orientation 2	merging *R* factor (%)	completeness $I > 0\sigma$	completeness $I > 1\sigma$	completeness $I > 2\sigma$
6.00	5.5	8.4	6.0	90.0	86.5	82.9
4.00	7.6	11.9	8.3	92.0	88.7	85.0
3.00	13.5	17.2	14.1	89.6	85.5	77.4
2.50	25.2	30.2	26.1	87.0	76.5	60.5
2.25	32.4	38.2	33.5	84.1	70.3	49.0
2.10	39.4	43.8	40.3	81.8	65.7	40.7
2.00	45.4	54.2	47.0	77.7	60.5	32.1
total			17.1			

The program TNT (Tronrud et al., 1987, Tronrud, 1992) was used for least squares refinement of this model *vs* the observed structure amplitudes from the mutant. After cycles of refinement against increasingly higher resolution data, new difference electron density maps were calculated. All of the side chains of the active site residues, the magnesium ion, and the side chain of Asn 270 could be placed unambiguously in the difference density and were added to the model. After further cycles of refinement, difference maps revealed the location of most of the residues in the flap. Next, refinement was performed on the model containing the flap, and new maps were generated. These maps were used to place the inhibitor at the active site and to locate potential water molecules in the structure. A final series of TNT calculations were performed to refine the parameters for (*S*)-atrolactate and to validate the selection of individual water molecules.

The final structure has an *R* factor of 19.0% *vs* all data from 20.0 to 2.1 Å resolution with intensities greater than 1σ (Table 2). The deviations from ideal geometry are all below the target values: the rms bond length deviation is 0.013 Å and the rms bond angle deviation is 1.7° (Table 3). This structure contains 2697 protein atoms, 1 magnesium atom, 12 inhibitor atoms, and 111 water molecules. The coordinates for this structure have been deposited in the Protein Data Bank at the Brookhaven National Laboratories.

Assay of MR Activity. The coupled spectrophotometric assay [utilizing (*S*)-mandelate dehydrogenase] and the polarimetric assay described by Mitra et al. (1995) were used to quantitate racemase activity.

Dependence of the Rate of Racemization on pH. The dependence of the rate of racemization on pH was evaluated using the polarimetric assay over the pH range from 5.5 to 10.25. The buffers used were MES, pH 5.5, 6.0, 6.5; PIPES, pH 6.5, 7.0, 7.5; HEPES, 7.5, 8.0, 8.5; TAPS, 8.5, 9.0; CHES, pH 9.0, 9.5, 10.0; and CAPS, pH 10.0, 10.25. Overlapping pH ranges were used to ensure that any discontinuities would be detected. The assay solutions contained 100 mM buffer and 10 mM $MgCl_2$. Each assay

Table 2: *R* Factor Report to 2.1 Å Resolution from TNT[a]

data set			count			rejected by resolution			% completeness		
observed			21566			2347			77		
calculated			25009			0			100		
Bragg spacing (Å)	5.66	3.94	3.33	2.98	2.74	2.56	2.42	2.31	2.22	2.14	total
reflections	2358	2241	2149	2028	1899	1850	1753	1701	1656	1584	19219
R factor (%)	0.20	0.13	0.16	0.19	0.20	0.21	0.21	0.22	0.23	0.25	0/190

[a] A total of 19219 matches were found. Resolution limits: 20.0−2.10 Å.

Table 3: Geometry Report from TNT

class	no.	mean	rms deviation from ideal values
bond length	2770	0.001 Å	0.013 Å
bond angle	3745	0.19°	1.7°
torsion angle[a]	1641	4.1 Å	25°
trigonal atom nonplanarity	59	−0.008 Å	0.012 Å
planar groups	404	−0.012 Å	0.014 Å
bad contacts	30	0.003 Å	0.003 Å
thermal parameter correlation	2753	0.17 Å^2	8.1 Å^2

[a] Torsion angles were not constrained during refinement.

was initiated by the addition of (*R*)- or (*S*)-mandelates to final concentrations of 100 or 150 mM. The pK_a values described by the data were determined using the program BELL (Cleland, 1979).

Solvent and Substrate Isotope Effects. Solvent isotope effects on k_{cat} were determined by comparing the rates of racemization of (*R*)- and (*S*)-[α-^{1}H]mandelates in 0.1 M HEPES buffer containing 3 mM $MgCl_2$ in either H_2O, pH 7.5, or D_2O, pD 7.5. The rates of the reaction were determined at 1, 3, and 7 mM concentrations of substrates; values for k_{cat} were then determined with the program HYPER.

Substrate isotope effects on k_{cat} were similarly determined by comparing the rates of racemization of (*R*)- and (*S*)-[α-^{1}H]mandelates and (*R*)- and (*S*)-[α-^{2}H]mandelates in 0.1 M HEPES, pH 7.5, containing 3 mM $MgCl_2$.

Exchange of the α-Protons of (R)- and (S)-Mandelates with D_2O. The rate of exchange of the α-proton of (*R*)- or (*S*)-mandelate with D_2O was measured at 30 °C with a 12 mM amount of each enantiomer in 20 mM HEPES, pD 7.5, containing 1 mM $MgCl_2$. Each reaction (0.73 mL) was initiated by the addition of enzyme (1.2 μg, wild type, D270N, or H297N) and monitored by recording successive ^{1}H NMR spectra with a Bruker AM-400 NMR spectrometer. The intensity of the resonance of the α-proton (4.9 ppm) was measured relative to the five aromatic protons (7.2−7.4 ppm), and the slope of the plot of intensity of the α-proton as a function of time was used to calculate the exchange rate.

Elimination of Bromide Ion from (R,S)-p-(Bromomethyl)-mandelate. The elimination of bromide ion from (*R,S*)-*p*-(bromomethyl)mandelate catalyzed by D270N was monitored as described by Kallarakal et al. (1995). Reactions (2.0 mL) were carried out in 100 mM NaMES, pH 6.0, containing 1 mM $Mg(NO_3)_2$ in both the presence and absence of D270N (6.0 mg). Each reaction was initiated by the addition of the substituted mandelate to a final concentration of 1 mM.

In a separate experiment, an analogous reaction was performed with 3.8 mg of D270N in a total volume of 1.5 mL. The reaction was initiated by the addition of the racemic substituted mandelate to a final concentration of 1 mM. At 6 min after the initiation of the reaction, the reaction was quenched by the addition of HCl to a final concentration of 0.6 M. The *p*-(methyl)benzoylformate and *p*-(hydroxymethyl)mandelate were isolated and quantitated as described by Kallarakal et al. (1995). The isolated amounts of *p*-(methyl)benzoylformate and *p*-(hydroxymethyl)mandelate were 0.57 and 0.62 μmol, respectively, for a total recovery of 79%. The enantiomeric purity of the *p*-(hydroxymethyl)-mandelate was determined by circular dichroism as described by Kallarakal et al. (1995).

RESULTS AND DISCUSSION

The experiments described in this article were designed to determine the importance of Asp 270 in influencing the catalytic properties of the structurally proximal His 297, the (*R*)-specific acid/base catalyst. Our hypothesis was that the carboxylate group of Asp 270 negates the positive electrostatic environment of the active site that is created by the ε-ammonium group of Lys 164 and the essential Mg^{2+}, thereby allowing the imidazolium group of His 297 to have a normal pK_a when (*R*)-mandelate is substrate.

Structural Characterization of D270N. The D270N mutant of MR was constructed and purified to apparent homogeneity as described in the Materials and Methods section. The mutant enzyme was crystallized in the presence of (*S*)-atrolactate and $(NH_4)_2SO_4$ as described previously for wild-type MR (Landro et al., 1994). The structure was solved to 2.1 Å resolution by difference Fourier analysis relative to the structure of wild-type MR refined to 2.0 Å resolution.

The active sites of wild-type MR and D270N are compared in Figure 1 (white structure, wild-type MR; yellow structure, D270N). The orientation of the carboxamide group of Asn 270 differs slightly from that observed for Asp 270 in wild-type MR ($\chi1 = 171°$ and $\chi2 = 124°$ in D270N; $\chi1 = 174°$ and $\chi2 = 103°$ in wild-type MR). This suggests that the carbonyl functionality of the carboxamide group of Asn 270 is hydrogen bonded to the peptidic NH groups of residues 272 and 273 (the distance to both NH groups is 2.9 Å in both structures) and that the amino group is oriented toward His 297. This slight reorientation is also characterized by a longer distance between the side chain of residue 270 and the N$^\delta$ of His 297 (2.7 Å in wild type MR and 3.2 Å in D270N). Coupled with these changes, the orientation of the imidazole group of His 297 also differs slightly from that observed for wild-type MR ($\chi1 = 180°$ and $\chi2 = 56°$ in D270N; $\chi1 = 175°$ and $\chi2 = 62°$ in wild-type MR).

This small structural perturbation (Figure 1) presumably is a consequence of the hydrogen bonding between the carboxamide group of Asn 270 and the imidazole group of His 297 relative to that between the carboxylate group of Asp 270 and His 297 in wild-type MR. As illustrated in

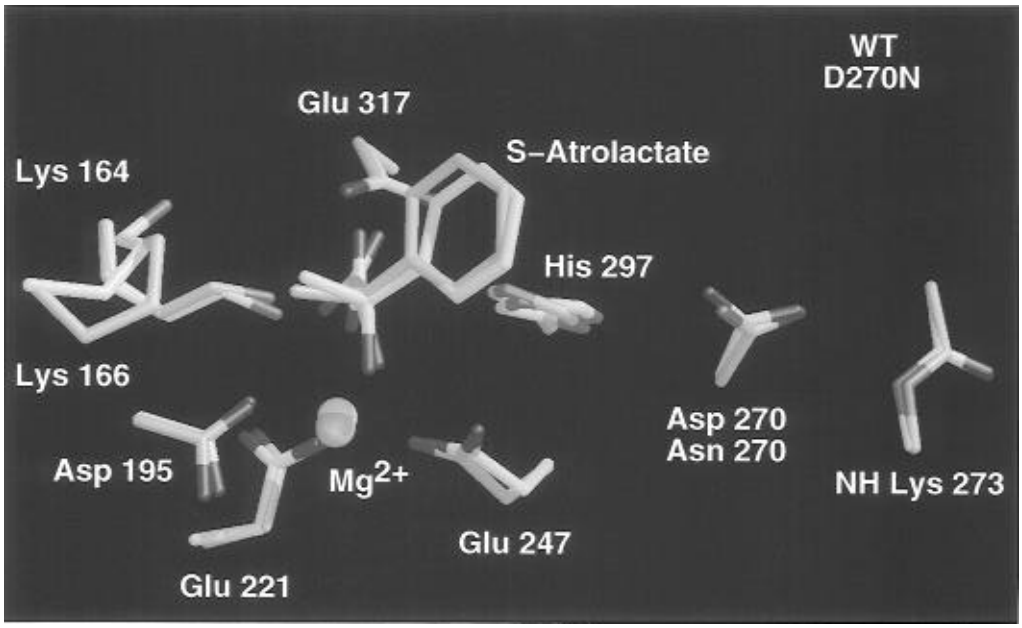

FIGURE 1: Superpositioning of the X-ray structures of the active site of wild-type MR with (*S*)-atrolactate bound in the active site (white; Landro et al., 1994) and of D270N with (*S*)-atrolactate bound in the active site (yellow). See the text for experimental details.

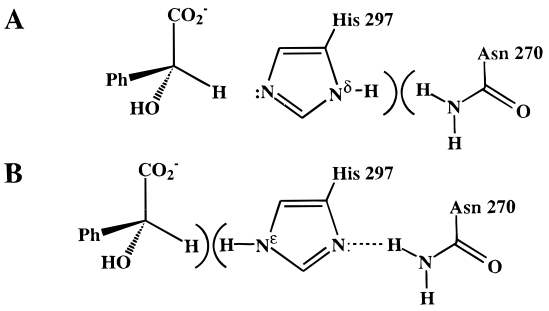

FIGURE 2: Two possible tautomeric structures for His 297 and their interaction with the amino moiety of the carboxamide group of Asn 270: (A) the δ-tautomer of His 297; (B) the ϵ-tautomer of His 297.

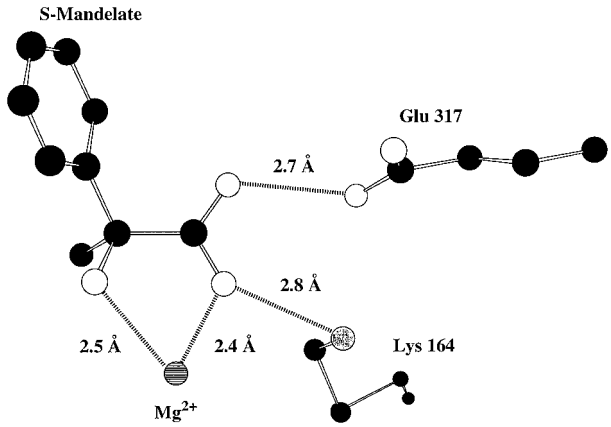

FIGURE 3: Interaction of (*S*)-atrolactate with the Mg^{2+} and the functional groups of Lys 164 and Glu 317 in the active site of D270N.

Figure 2, the hydrogen bonding between His 297 and Asn 270 will be determined by the tautomeric form of the imidazole group. In the δ-tautomer that is necessarily present in the active site of wild-type MR, the carboxylate group of Asp 270 is hydrogen bonded to the $N^{\delta}-H$, thereby orienting this group in the active site. If this tautomer is also present in the active site of D270N (panel A), the $N^{\delta}-H$ and the amino group of the carboxamide group of Asn 270 will sterically clash, thereby providing an explanation for the observed structural perturbation. As a consequence of this change in geometry we assume that the α-proton of bound substrate will not be in the plane of the imidazole/imidazolium functional group of His 297; i.e., the geometry is not amenable for facile transfer of a proton between substrate, the enolic intermediate, and the functional group of His 297. This situation is analogous to that observed for the Lys to Arg substitution in the active site of K166R (Kallarakal et al., 1995).

In contrast, if the ϵ-tautomer of His 297 is present in the active site of D270N (Figure 2, panel B), the amino group of the carboxamide group of Asn 270 should function as a hydrogen bond donor to N^{δ} of His 297. While this hydrogen bond should be a structurally conservative replacement for the Asp 270−His 297 hydrogen bond pair that is present in the active site of wild-type MR, it is expected to be catalytically unproductive since the N^{ϵ} of His 297 would be protonated and, therefore, unable to either abstract the α-proton from (*R*)-mandelate to generate the enolic intermediate or donate a proton to the enolic intermediate generated by abstraction of the α-proton from (*S*)-mandelate by Lys 166 to generate (*R*)-mandelate.

(*S*)-Atrolactate is coordinated to the essential Mg^{2+} in the active site of D270N (Figure 3) by both its hydroxyl group (2.5 Å) and one of its carboxylate oxygens (2.4 Å). The carboxylate oxygen of the inhibitor that is coordinated to Mg^{2+} is also hydrogen bonded to the ϵ-ammonium group of Lys 164 (2.8 Å) in the active site of D270N. Within the estimated errors, these distances are identical to those observed for wild-type MR complexed with (*S*)-atrolactate (Landro et al., 1994)). Thus, neutralization of the negative charge of the carboxylate group of the bound inhibitor, and, by analogy, substrate, should be unchanged in the D270N mutant.

The carboxylic acid group of Glu 317 both functions as a general acid catalyst that transfers a proton toward the carboxylic group of the substrate as the α-proton is abstracted and stabilizes the resulting enolic intermediate by participa-

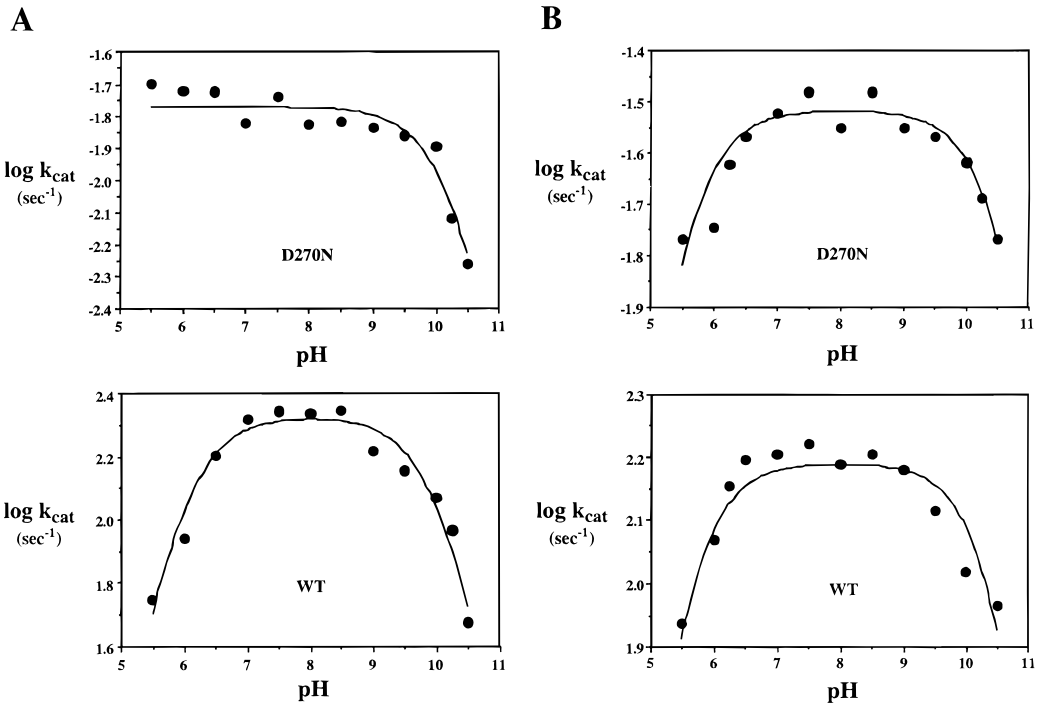

FIGURE 4: Dependence of k_{cat} on pH for D270N (top) and wild-type MR (bottom): panel A, (*R*)-mandelate as substrate; panel B, (*S*)-mandelate as substrate. See text for experimental details.

ting in a short, strong hydrogen bond to the OH group of the intermediate (Mitra et al., 1995). In the active site of D270N (Figure 3), the carboxylate oxygen of (*S*)-mandelate that is not coordinated to the essential Mg^{2+} is hydrogen bonded to the carboxylic acid group of Glu 317, as judged by the O−O distance between the bound substrate and the functional group (2.6 Å). Within error, this distance is identical to that observed for the analogous hydrogen bond involving the carboxylic acid group of Glu 317 in the active site of wild-type MR (2.8 Å; Landro et al., 1994).

Thus, the only observable difference in the active site of D270N relative to wild-type MR is the displacement of His 297 that results from substitution of the carboxamide functional group of asparagine for the carboxylate group of aspartate at residue 270. As a result, any changes in catalytic activity can be associated with (1) the reorientation of His 297 by the substitution at residue 270 and (2) the influence of the charge of the functional group of residue 270 on the ionization behavior of His 297.

Mandelate Racemase Activity of D270N. The values of k_{cat} measured for wild-type MR and the D270N mutant at pH 7.5 using (*R*)- and (*S*)-mandelate as substrate were determined using the polarimetric assay; the value in the (*R*)- to (*S*)-direction is 0.018 ± 0.003 s^{-1}, and the value in the (*S*)- to (*R*)-direction is 0.037 ± 0.004 s^{-1}. With either enantiomer of the substrate, the k_{cat} values are reduced by ~10^4-fold from the values measured for wild-type MR.

The values for K_m for the racemization reactions catalyzed by D270N cannot be measured using the polarimetric assay since at low concentrations of mandelate the signal amplitude is inadequate for accurate quantitation of optical rotation. The coupled assay [using (*S*)-mandelate dehydrogenase to measure spectrophotometrically the rate of production of (*S*)-mandelate] is sensitive at low concentrations of mandelate and was used to measure the K_m for (*R*)-mandelate. The value measured for the K_m in the (*R*)- to (*S*)- direction is 1.5 mM. From the Haldane equation, the value for the K_m in the (*S*)- to (*R*)-direction can be calculated to be 2.1 mM.

Dependence of k_{cat} on pH. The dependence of k_{cat} on pH using each enantiomer of mandelate as substrate is compared for wild-type MR and D270N in Figure 4 [panel A, (*R*)-mandelate substrate; panel B, (*S*)-mandelate substrate].

For D270N using (*R*)-mandelate as substrate, the data can be described by a low pH plateau that decreases at high pH as described by a pK_a of 10.2 ± 0.10 for the descending limb. This dependence of k_{cat} on pH deviates from that observed for wild-type MR in that the low pH ascending limb is absent. This difference suggests that the pK_a of His 297 [the (*R*)-specific base] is depressed in the active site of D270N as would be expected if Asp 270 influenced the pK_a of His 297.

For D270N using (*S*)-mandelate as substrate, the data are described by a pK_a of 5.6 ± 0.09 for the ascending limb and a pK_a of 10.1 ± 0.09 for the descending limb. Inspection of Figure 4 reveals that these values do not differ significantly from those that describe the dependence of k_{cat} on pH for wild-type MR.

Taken together these data support the proposed role of Asp 270 in negating the positive electrostatic potential in the active site of wild-type MR so that the imidazolium group of His 297 can have a normal pK_a when it abstracts the α-proton from (*R*)-mandelate.

Substrate and Solvent Kinetic Isotope Effects. Substrate, solvent, and combined substrate/solvent kinetic isotope effects were measured in both the (*S*)- to (*R*)- and (*R*)- to (*S*)-directions. In the (*S*)- to (*R*)-direction, the substrate deuterium isotope effect was indistinguishable from unity (1.0 ± 0.1); the solvent deuterium isotope effect was 2.0 ± 0.3; and the combined substrate/solvent deuterium isotope effect was 2.2 ± 0.3. These data are in accord with the rate-limiting transition state being the conversion of the enolic intermediate to (*R*)-mandelate and not involving the abstraction of the substrate α-proton of (*S*)-mandelate.

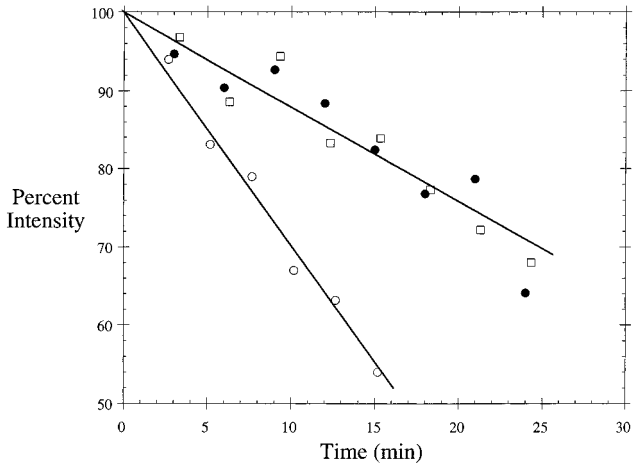

FIGURE 5: Time dependence of the exchange of the α-proton of (*S*)-mandelate with solvent catalyzed by wild-type MR (○), H297N (□), D270N (●). See text for experimental details.

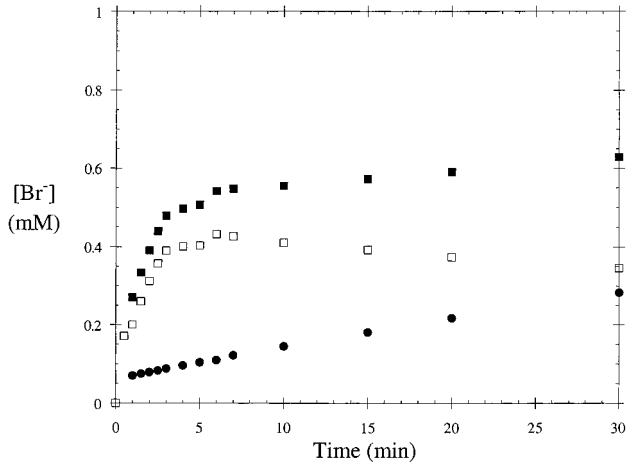

FIGURE 6: Time dependence of the elimination of bromide ion from (*R,S*)-*p*-(bromomethyl)mandelates catalyzed by D270N: total bromide ion released, ■; nonenzyme-catalyzed bromide ion release, ●; enzyme-catalyzed bromide ion release, □.

Unexpectedly, in the (*R*)- to (*S*)-direction, the substrate deuterium isotope effect was indistinguishable from unity (0.9 ± 0.1); the solvent deuterium isotope effect was 2.5 ± 0.3; and the combined substrate/solvent deuterium isotope effect was 2.0 ± 0.3. In the (*R*)- to (*S*)-direction the rate-limiting transition state should be the conversion of (*R*)-mandelate to the enolic intermediate, and the rates should be subject to significant substrate and solvent isotope effects due to general basic and general acidic catalysis, respectively. That no substrate isotope effect could be detected may be the result of a suboptimal geometry for the abstraction of the α-proton of (*R*)-mandelate due to the reorientation of His 297 by the Asp to Asn substitution (Westheimer, 1961). This finding does not alter our conclusions (*vide infra*) regarding the role of Asp 270 in influencing the pK_a of His 297.

Exchange of the α-Proton of (S)-Mandelate Catalyzed by D270N. The exchange of the α-proton with solvent deuterium catalyzed by D270N, H297N, and wild-type MR was monitored by ^{1}H NMR spectroscopy as described in the Materials and Methods section (Figure 5). Wild-type MR and H297N were observed to catalyze the exchange of the α-proton of (*S*)-mandelate with solvent at rates of 150 and 60 s^{-1}, respectively; these values are in excellent agreement with those reported previously (Landro et al., 1991). D270N was also observed to catalyze the exchange of the α-proton of (*S*)-mandelate with solvent at a rate of 60 s^{-1}. No exchange of the α-proton of (*R*)-mandelate with solvent could be detected for either D270N or H297N.

The identical exchange rates measured for D270N and H297N indicate that, despite the structural perturbation observed in the active site of D270N involving His 297, the ϵ-amino group of Lys 166 retains its ability to catalyze facile suprafacial exchange of the α-proton with solvent.

Elimination of Bromide Ion from (R,S)-p-(Bromomethyl)-mandelate. The H297N mutant of MR catalyzes the stereospecific elimination of bromide ion from (*S*)-*p*-(bromomethyl)mandelate at a rate (0.012 s^{-1}) that is approximately one-half that observed for wild-type MR (Landro et al., 1991; A. T. Kallarakal and J. A. Gerlt, unpublished observations). In contrast, the K166R mutant of MR catalyzes the stereospecific elimination of bromide ion from (*R*)-*p*-(bromomethyl)mandelate at a rate (0.012 s^{-1}) that is also approximately one-half that observed for wild-type MR (Kallarakal et al., 1995). The absolute and opposite stereospecificities observed in these reactions were used as evidence that His 297 is the (*R*)-specific acid/base catalyst and that Lys 166 is the (*S*)-specific acid/base catalyst.

We have studied both the rate and stereospecificity of the elimination of bromide ion from (*R,S*)-*p*-(bromomethyl)-mandelate catalyzed by D270N. As shown in Figure 6, D270N catalyzes the rapid elimination of bromide ion from approximately one-half of the racemic mixture of the substituted mandelate. After approximately 5 min, the slower release of bromide ion is that associated with (nonenzymatic) solvolysis of the inert enantiomer of *p*-(bromomethyl)-mandelate to form *p*-(hydroxymethyl)mandelate. The rate of the enzyme-catalyzed elimination reaction is 0.014 s^{-1}. This value is similar to those reported for the elimination reactions catalyzed by H297N (Landro et al., 1991) and K166R (Kallarakal et al., 1995).

The absolute configuration of the inert enantiomer of *p*-(bromomethyl)mandelate was determined as described in the Materials and Methods section. The circular dichroic spectra that were obtained for equal concentrations (0.072 mM) of authentic (*R*)-*p*-(hydroxymethyl)mandelate (spectrum A), the product of the D270N-catalyzed reaction (spectrum B), and racemic *p*-(hydroxymethyl)mandelate (spectrum C) are shown in Figure 7. From inspection of these spectra, the inert enantiomer of *p*-(bromomethyl)mandelate has the (*R*)-configuration, indicating that D270N catalyzes the stereospecific elimination of bromide ion from (*S*)-*p*-(bromomethyl)mandelate. The enantiomeric excess of (*R*)-*p*-(hydroxymethyl)mandelate was 76%.

We conclude that, in the active site of D270N, Lys 166 retains its ability to catalyze the facile abstraction of the α-proton from (*S*)-*p*-(bromomethyl)mandelate, and, by analogy, (*S*)-mandelate, at a rate that is indistinguishable from the proton abstraction catalyzed by Lys 166 in the active site of wild-type MR. Thus, despite the fact that the position of His 297 has been altered as a result of the Asp to Asn substitution at residue 270, Lys 166 in the presence of the electrophilic catalyst Glu 317 (Mitra et al., 1995) retains its ability to function as the (*S*)-specific acid/base catalyst.

Conclusions. The experiments described in this paper suggest that His 297 and Asp 270 are functioning together as a catalytic dyad in the active site of wild-type MR, in

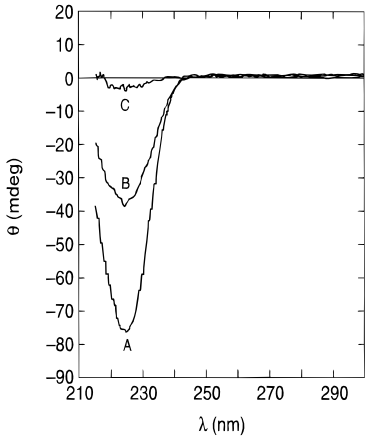

FIGURE 7: Circular dichroic spectra of authentic (*R*)-*p*-(hydroxymethyl)mandelate (A), the *p*-(hydroxymethyl)mandelate produced by the elimination of bromide ion from (*R*,*S*)-*p*-(bromomethyl)-mandelates in the presence of D270N (B), and racemic *p*-(hydroxymethyl)mandelate (C).

analogy to those observed for a number of mechanistically unrelated enzymes, e.g., trypsin (Craik et al., 1987), phospholipase A_2 (Dijkstra et al., 1981), malate and lactate dehydrogenases (Birktoft & Banaszak, 1983), and various zinc containing enzymes (Christianson & Alexander, 1989). The hydrogen-bonding interaction between Asp 270 and His 297 in wild-type MR is likely to be important in positioning the imidazole group of His 297 appropriately for facile abstraction of the α-proton of (*R*)-mandelate. The data also are consistent with the hypothesis that the negative charge of Asp 270 is responsible for "insulating" His 297 from the positive electrostatic potential that appears to lower the pK_a of the ϵ-ammonium group of Lys 166 from its normal value.

REFERENCES

Birktoft, J. J., & Banaszak, L. J. (1983) *J. Biol. Chem. 258*, 472−482.

Bruice, T. C., & Schmir, G. L. (1959) *J. Am. Chem. Soc. 81*, 4552−4559.

Christianson, D. W., & Alexander, R. S. (1989) *J. Am. Chem. Soc. 111*, 6412−6419.

Cleland, W. W. (1979) *Methods Enzymol. 63*, 103−138.

Craik, C. S., Rozniak, S., Largman, C., & Rutter, W. J. (1987) *Science 237*, 909−913.

Creighton, T. E. (1993) *Proteins: Structure and Molecular Properties*, p 6, W. H. Freeman, New York.

Dijkstra, B. W., Drenth, J., Kalk, K. H., & Hartley, B. S. (1981) *Nature 289*, 604−606.

Gerlt, J. A., Kenyon, G. L., Neidhart, D. J., Petsko, G. A., & Powers, V. M. (1992) *Curr. Opin. Struct. Biol. 2*, 736−742.

Highbarger, L. A., Kenyon, G. L., & Gerlt, J. A. (1996) *Biochemistry 35*, 41−46.

Kabsch, W. (1988a) *J. Appl. Crystallogr. 21*, 67−71.

Kabsch, W. (1988b) *J. Appl. Crystallogr. 21*, 916−924.

Kallarakal, A. T., Kozarich, J. W., Gerlt, J. A., Clifton, J. R., Petsko, G. A., & Kenyon, G. L. (1995) *Biochemistry 34*, 2788−2797.

Kenyon, G. L., & Hegeman, G. D. (1979) *Adv. Enzymol. Relat. Areas Mol. Biol. 50*, 325−360.

Knowles, J. R. (1976) *Crit. Rev. Biochem. 4*, 165−173.

Kokesh, F. C., & Westheimer, F. H. (1971) *J. Am. Chem. Soc. 93*, 7270−7274.

Landro, J. A., Kallarakal, A. T., Ransom, S. C., Gerlt, J. A., Kozarich, J. W., Neidhart, D. J., & Kenyon, G. L. (1991) *Biochemistry 30*, 9274−9281.

Landro, J. A., Gerlt, J. A., Kozarich, J. W., Koo, C. W., Shah, V. J., Kenyon, G. L., Neidhart, D. J., Fujita, S., & Petsko, G. A. (1994) *Biochemistry 33*, 635−643.

Laursen, R. A., & Westheimer, F. H. (1966) *J. Am. Chem. Soc. 88*, 3426−3430.

Lin, D. T., Powers, V. M., Reynolds, L. J., Whitman, C. P., Kozarich, J. W., & Kenyon, G. L. (1988) *J. Am. Chem. Soc. 110*, 323−324.

Mitra, B., Kallarakal, A. T., Kozarich, J. W., Gerlt, J. A., Clifton, J. R., Petsko, G. A., & Kenyon, G. L. (1995) *Biochemistry 34*, 2777−2787.

Neidhart, D. J., Howell, P. L., Petsko, G. A., Powers, V. M., Li, R., Kenyon, G. L., & Gerlt, J. A. (1991) *Biochemistry 30*, 9264−9273.

Petersen, D. J., & Bennett, G. N. (1990) *Appl. Environ. Microbiol. 56*, 3491−3498.

Powers, V. M., Koo, C. W., Kenyon, G. L., Gerlt, J. A., & Kozarich, J. W. (1991) *Biochemistry 30*, 9255−9263.

Schmidt, D. J., & Westheimer, F. H. (1971) *Biochemistry 10*, 1249−1253.

Tronrud, D. E. (1992) *Acta Crystallogr. A48*, 912−916.

Tronrud, D. E., Ten Eyck, L. F., & Matthews, B. W. (1987) *Acta Crystallogr. A43*, 489−501.

Westheimer, F. H. (1961) *Chem. Rev. 61*, 265.

BI960174M